Journal of Inorganic and General Chemistry / Zeitschrift für anorganische und allgemeine Chemie
Volume 643, Issue 18, October 2017, pp. 1167-1172
DOI: 10.1002/zaac.201700244

Formation and Structural Characterization of Metal Complexes derived from Thiosalicylic acid

Minu G. Bhowon[a*], Sabina Jhaumeer-Laulloo[a], Salma Moosun[a], Lisa Humphreys[c], Simon Coles[b], Roshni Fowdram[a], Evena Mungra[a],

[a]*Department of Chemistry, Faculty of Science, University of Mauritius, Mauritius*

[b]*Chemistry, Faculty of Natural & Environmental Sciences, University of Southampton, UK*

[c]*Centre for Defence Chemistry, Cranfield University, Defence Academy of the United Kingdom, Shrivenham, SN6 8LA, UK*

Corresponding author email: mbhowon@uom.ac.mu

Tel: +230 4037502

Abstract

The formation and structural aspects of some metal complexes of thiosalicylic acid (TSA) were studied. The μ-bridging tetra-coordinated Ru complex, $[Ru(C_6H_4(CO_2)(\mu\text{-}S)(H_2O)]_2$ (**1**) was formed by hydrothermal reaction of TSA with $RuCl_3$. The complexes $[M(dtdb)(phen)(H_2O)]_n$ (**2**-**4**) (M= Zn(II), Co(II), Ni(II), dtdb = 2,2'-dithiodibenzoate anion, phen = 1,10-phenanthroline) were obtained by the slow diffusion technique and the *in situ* S-S bond formation was confirmed by elemental, spectral and X-ray analysis. Reaction of TSA with $CuCl_2$ and 2,2'-bipyridine (bipy) under the slow diffusion technique yielded the dimer [Cu(tdb)(bipy)] (**5**) (tdb = thiodibenzoic acid) where the in-situ generation of 2,2'-thiodibenzoic acid was observed.

Keywords: thiosalicylic acid, dithiodibenzoic acid, thiodibenzoic acid, X-ray

1.0 Introduction

Aryl sulfides are fundamental building blocks which have the capacity to coordinate with metal atoms to form different structural frameworks, exhibiting interesting biological and catalytic activities [1-3]. The coordination chemistry of aryl sulfides containing both oxygen and sulfur donor atoms is of interest as the presence of both hard carboxylate and soft thiolate donors allow a wide range of complexes with a variety of coordination modes. Thiosalicylic acid (TSA) gives rise to various chelating frameworks using either sulfur/oxygen or both donor atoms depending on the metal used and the reaction conditions [4]. TSA metal complexes can adopt various binding modes where (i) S coordinates leaving the carboxylic acid free [5] (ii) carboxylate anion

binds in a monodentate fashion together with sulfur coordination [6] (iii) both S and O coordinate [7, 8] (iv) carboxylate anion binds in a bidentate manner with [9] or without S coordination [10]. Binuclear or trinuclear complexes of ruthenium are reported with TSA where ruthenium binds via an S,O chelating mode through thiolate bridging [11-13]. The reaction of TSA with metal salts such as Co and Zn gave polymeric complexes where monodentate or bidentate carboxylate binding together with sulfur coordination has been reported [8, 14].

It is known that in highly acidic condition, TSA remains unchanged while at pH 6, 50 % of the TSA is oxidized to its disulfide derivative, dtdb. At pH 7, complete oxidation to a disulfide derivative is observed [15, 16]. Murugavel *et al.* [17] reported the oxidative coupling reaction of TSA to dtdb in the presence of heavier alkaline earth metals giving rise to polymeric solids of the formulae $[\{M(dtdb)(H_2O)_2\}.0.5(C_2H_5OH)]_n$ (M= Ca, Sr) and$[\{Ba_2(dtdb)_2(H_2O)_2\}.0.5H_2O]_n$. Dtdb coordinates to Ca^{2+} and Sr^{2+} ions via carboxylate anion while the disulfide coordination was observed for Ba ions only.

In continuation of our interest in metal sulfur compounds, we herein report the synthesis of metal complexes derived from thiosalicylic acid where it behaves either as a SO donor or it is chemically oxidized to diaryl disulfides/sulfides prior to coordination to metals.

2.0 Experimental Section

2.1 Materials and Methods

2.1.1 Chemicals used

All chemicals namely thiosalicylic acid, 2,2'-bipyridine, 1,10-phenanthroline monohydrate, copper(II) chloride dihydrate, ruthenium(III) chloride trihydrate, cobalt(II) chloride, zinc(II) chloride, nickel(II) chloride, methanol, diethyl ether, dimethyl sulfoxide, dimethyl formamide, acetonitrile were purchased from either Aldrich, Sigma, BDH, Fischer Scientific, Alpha Chemika or Acros Organics and were used without further purification.

2.1.2 Equipment used

IR spectra (solid) using diamond cell were recorded on an Alpha Bruker FTIR spectrophotometer in the range of 4000-400 cm^{-1}. ^1H NMR and ^{13}C NMR were recorded using a Bruker Spectrospin 250 MHz NMR Spectrometer. Melting points were determined on a Stuart Scientific Digital Melting point Apparatus. Elemental analyses were obtained from a EuroVector EA-3000

Elemental Analyser and pH was recorded on Martini Instruments Mi160 Bench Temperature/Ph Meter. Ruthenium content was determined using a GBC Avanta AAS (Atomic Absorption Spectrometer). Conductivity was measured using a Jenway 4510 Conductivity Meter.

2.2 Synthesis of Ru complex (1)

A mixture of $RuCl_3.3H_2O$ (0.187 g, 0.715 mmol) and TSA (0.220 g, 1.44 mmol) in water (20 mL) was refluxed for 6 hours with dropwise addition of 1 M NaOH after every 15 min. After cooling to room temperature, the solution was filtered and the resulting dark brown precipitate obtained as residue was washed with water, methanol and diethyl ether.

$[C_{14}H_{12}O_6S_2Ru_2]$ (1): Yield 82.3%, M.p. > 300 °C. Anal. Found(calcd): C 31.36 (30.97); H 2.31 (2.21); S, 11.84 (11.84); Ru 38.14 (37.28). Calc.: 30.97; H, 2.21; S, 11.84; Ru 37.28 %. **IR**: ν = 3345 (νO-H), 1578 (νCOO asym), 1357 (νCOO sym), 963 (νC-S) cm^{-1}. **^{1}H-NMR** (DMSO-d_6): δ = 8.0 (dd, 2H; 6 Hz, 1 Hz), 7.9 (bd, 1H), 7.6 (dd, 1H; 6 Hz, 1 Hz), 7.5 (td, 2H; 6 Hz, 1 Hz), 7.3 (td, 2H; 6 Hz, 1.9 Hz) ppm. ^{13}C-NMR (DMSO-d_6): δ =162.8, 139.4, 133.8, 132.1, 131.4, 130.2, 128.5, 126.5, 125.5 ppm.

2.3 Synthesis of Zn, Co, Ni and Cu complexes by slow diffusion method (2-5)

A solution of the metal chloride (0.708 mmol) in methanol (5 ml) was carefully layered over a mixture of TSA (0.701 mmol) and bipy/phen (0.701 mmol) in DMF (5 ml). The pH of TSA was adjusted to 7.21 with 1 M NaOH. After 3-5 weeks, the desired product formed in the reaction mixtures was collected and washed with methanol, ether and dried.

2.3.1 $[C_{29}H_{25}O_6N_3S_2Zn]$ (2): pale orange crystals; Yield 46.0%; M.p. > 300 °C. Anal. Found (calcd): C 54.53 (54.33); H 3.46 (3.93), N 6.15 (6.55), S 10.50 (10.00) %. **IR**: 3220 (νO-H), 1578 (νCOOasym), 1372 (νCOOsym), 961(νC-S), 642 (νZn-N), 557 (νZn-O), 472 (νS-S) cm^{-1}.

2.3.2 $[C_{29}H_{25}O_3N_3S_2Co]$ (**3**): black crystals; Yield 40.0%; M.p. > 300 °C. Anal. Found (calcd): C 55.42 (54.89); H 3.52 (3.97); N 5.45 (6.62); S 10.23 (10.11) %. **IR**: 3270 (νO-H), 1569 (νCOOasym), 1372 (νCOOsym), 961 (νC-S), 608 (νCo-N), 518 (νCo-O), 472 (νS-S) cm^{-1}.

2.3.3 [$C_{29}H_{25}O_6N_3S_2Ni$] (4): green powder; Yield 47.0%; M.p. > 300 °C. Anal. Found (calcd): C 55.02 (54.91); H 3.59 (3.97); N 6.90 (6.62); S 10.35 (10.11) %. **IR**: $\nu_{O-H,}$ 3327, $\nu_{COOasym}$, 1586, $\nu_{COOsym,}$ 1385, ν_{C-S} 956, ν_{Ni-N}, 653, $\nu_{Ni-O,}$ 550, $\nu_{S-S,}$ 476 cm^{-1}

2.3.4 [$C_{24}H_{16}O_4N_2SCu_2$] (5): dark blue crystals; Yield 33.0%; M.p. 260 °C. Anal. Found (calcd): C 58.05 (58.59); H 3.42 (3.28); N 5.91 (5.69); S 6.99 (6.52) %. **IR**: 3058 (νC-H), 1580 (νCOOasym), 1368 (νCOOsym), 492 (νCu-O), 437 (νCu-N) cm^{-1}.

2.4 X-ray Crystallography

Single-crystal X-ray diffraction data for **2**, **3** and **5** were collected at 100K on a Rigaku AFC12 goniometer equipped with an enhanced sensitivity (HG) Saturn 724+ detector mounted at the window of an FR−E+ Superbright Mo Kα rotating anode generator with optics (VHF Varimax 70μm focus for **2** and **3** and HF Varimax 100μm focus for **5)** and an Oxford Cryosystems Cobra cooling device [18].

Cell determination, data collection, data reduction, cell refinement and absorption corrections were carried out using CrystalClear-SM Expert 3.1 b27 software [19]. Data reduction, cell refinement and absorption corrections were carried out using CrysAlisPro for structures **2** and **3**. Structures **2**, **3** and **5** were solved using Superflip [20]. All structures were refined using full-matrix least-squares refinements in the SHELX2013 software [21]. All non-hydrogen atoms were refined with anisotropic displacement parameters. All hydrogen atoms were added at calculated positions and refined using a riding model with isotropic displacement parameters based on the equivalent isotropic displacement parameter (Ueq) of the parent atom. A disordered DMF solvent molecule was present in structure (**2).** This was modelled over two positions, one accounting for 65% of its chemical occupancy and the other 35%. Figures 2, 4 and 5 were drawn using Olex2 [22]. The data quality of structure (**3**) was poor and therefore a confident full structure determination could not be achieved. Hence, only a brief description of the rough connectivity of the structure will be described.

3.0 Results and discussions

The reaction of $RuCl_3.3H_2O$ and TSA under hydrothermal conditions led to the formation of a brown powder, $[Ru(C_6H_4(CO_2)(\mu\text{-}S)(H_2O)]_2$ (**1**) (Scheme 1). Complex (**1**) was found to be soluble in DMF and DMSO but insoluble in other common organic solvents. Molar conductivity of (**1**) suggested the non-electrolytic nature of the complex. When the same reaction was carried out by the slow diffusion of TSA and bipy in DMF into methanolic solution of $RuCl_3.3H_2O$, no product was isolated. In the IR spectrum of **(1)**, the two peaks at 1578 and 1357 cm^{-1} ($\Delta\nu$ = 221 cm^{-1}) were assigned to the asymmetric and symmetric stretching COO^- vibration, indicating monodentate type of bonding [23]. The absence of the peak at 2516 cm^{-1} indicated the deprotonation of SH followed by coordination with Ru. The band at 963 cm^{-1} was attributed to ν(C-S) [24] while the broad peak at 3345 cm^{-1} was due to ν(O-H) vibration of the solvated/coordinated water molecules.

Absence of the peak at 9-10 ppm in ^{1}H NMR indicated the deprotonation of carboxylic group prior to coordination. The resonances due to the aromatic protons appeared in the range of δ 8.0-7.3 ppm. The ^{13}C-NMR spectrum showed the aromatic carbon atoms at δ 125 – 139 ppm and the peak at δ 162 ppm was due to carboxylic carbon.

From the elemental and spectral analyses, it could be deduced that complex (**1**) has a Ru_2S_2 units formed by two bridging thiolates. These types of ruthenium coordinating frameworks have been reported earlier [11].

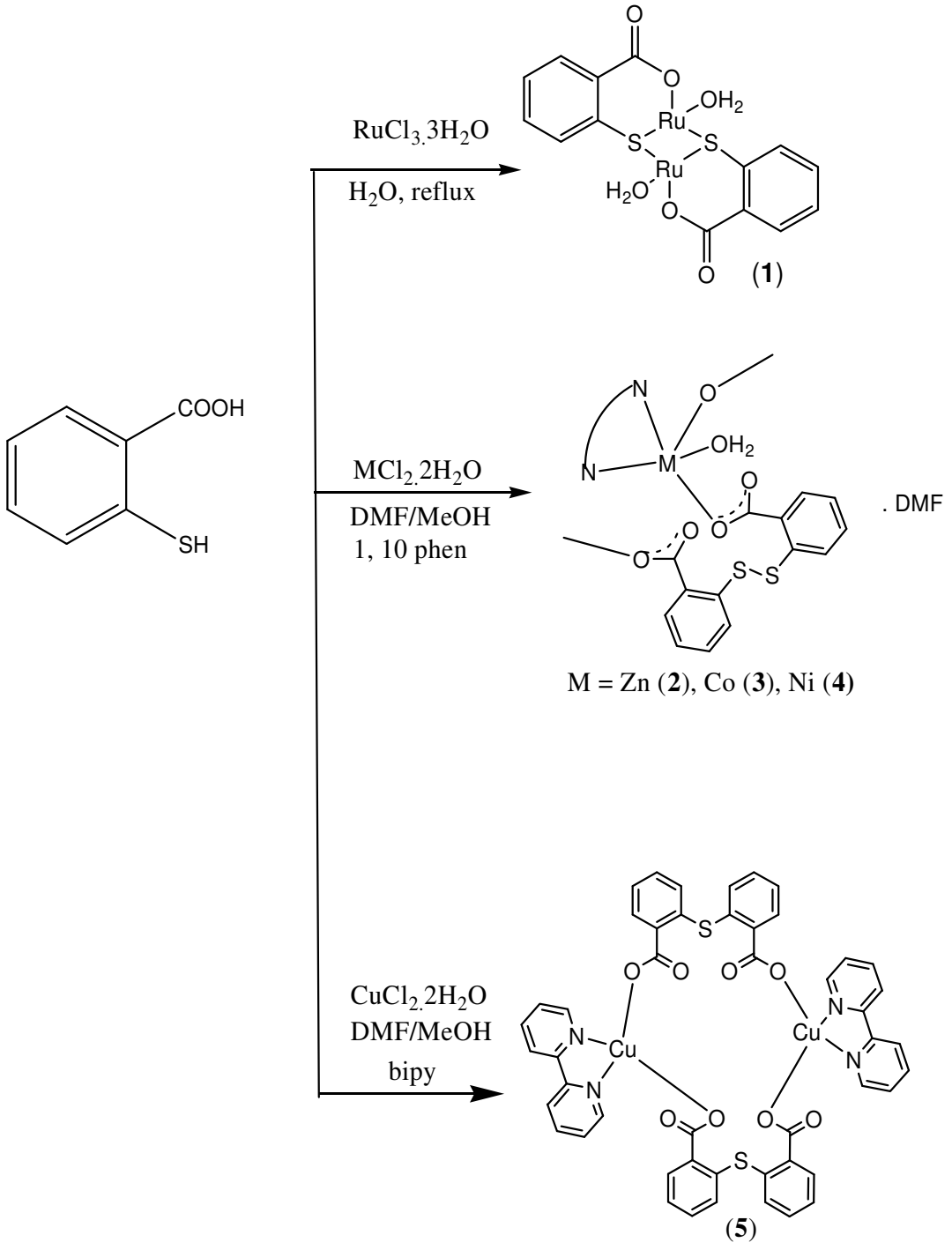

Scheme 1: Synthesis of metal complexes derived from TSA

Dai *et al*. has reported the formation of the dimeric complex $[Zn(SC_6H_4CO_2)(phen)]_2$ by the reaction of $ZnCl_2$ with TSA in the presence of phen where each Zn is in distorted octahedral

geometry with bidentate carboxylate together with sulfur co-ordination [25]. However, in the present study, the reaction of metal salts such as $ZnCl_2$, $CoCl_2$ and $NiCl_2$ with thiosalicylic acid in the presence of phen under slow diffusion yielded complexes having the formula $[M(dtdb)(phen)(H_2O)]_n$.DMF (**2-4**) (Scheme 1). The formation of (**2-4**) was dependent on the *in-situ* oxidation of the TSA to form disulfide S-S bridges. The oxidative coupling of TSA to dtdb has been reported earlier [26]. It is proposed that TSA is doubly deprotonated generating the species $(C_6H_4(CO_2)S)^{2-}$ and the pair of thiolate ions are oxidized forming the 2,2'-dithiodibenzoate ion, as shown in Scheme 2. Formation of dtdb is confirmed by X-ray data analysis of **2**.

The difference between the asymmetrical (1586-1583 cm^{-1}) and symmetrical stretching COO^- (1372-1385 cm^{-1}) ($\Delta\nu$ = 214 - 199) vibrations in complexes (**2**-**4**) showed that the carboxylate bonded to the metal ion in a monodentate fashion. The absence of the S-H bond and the presence of new band at 472-476 cm^{-1} suggested the formation of S-S bond. The presence of intense peak in the region of 714-717 cm^{-1} was due to C-S bond. The presence of bands in the region 500-650 corresponded to Zn-O (557) [27], Zn-N (642), Ni-N (653), Ni-O (550), Co-N (608) [28] and Co-O (518).

When $CuCl_2$ was reacted with TSA in the presence of bipy, a green powder $[Cu(bipy)Cl_2]$ and dark blue crystals of the dimeric complex $[Cu_2(tdb)_2(bipy)_2]$ (**5**) (tdb = thiodibenzoic acid) were isolated. In complex **5**, rearrangement of TSA to tdb was observed. This could be due to the oxidation of TSA to dtdb followed by extrusion of sulfur resulting in the formation of tdb prior to coordination to copper (Scheme 2). Although the conversion of dtdb to tdb in the presence of metal salt has been reported earlier [29], this is the first time the *in-situ* generation of thiodibenzoic acid from TSA, followed by coordination to copper metal has been observed. A similar complex has previously been reported which was synthesized through a different reaction pathway [23, 30]. The slight difference between the reported structure and complex (**5**) is the absence of coordinated water molecules and solvent water in complex (**5**) leading to different packing arrangements of the material. Selected bond lengths and angles are given in Table 2. The values noted are in good agreement with previously reported data [23]. Similar reaction in the presence of phen yielded only $[Cu(phen)Cl_2]$.

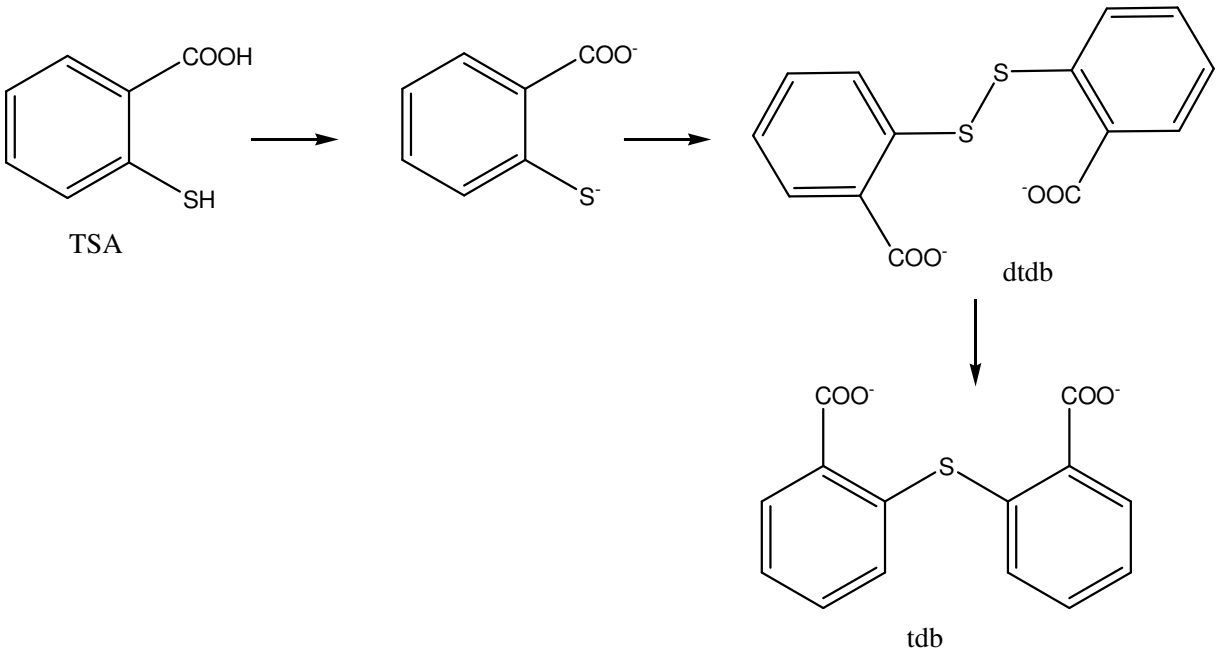

Scheme 2: *In-situ* reaction of TSA

3.1 X-ray structures (2), (3) and (5)

Polymeric complex (**2**) $[Zn_2(dtdb)_2(phen)_2(H_2O)_2]DMF$ crystallizes in the monoclinic centrosymmetric space group *P*121/*n*1. A perspective view of the X-ray structure of (**2**) with the polymeric network is shown in Figure 1 while the refinement parameters of selected bond lengths and bond angles are given in Tables 1 and 2.

Table 1 Data collection and refinement parameters for the crystal structures of (**2**) and **(5)**

Identification code	**2**	**5**
Empirical formula	$C_{55}H_{43}N_5O_{11}S_4Zn_2$	$C_{48}H_{32}Cu_2N_4O_8S_2$
Formula weight	1208.92	983.97
Temperature (K)	100 K	100 K
Wavelength (Å)	0.71073 Å	0.71073 Å
Crystal system	Monoclinic	Triclinic
Space group	*P*121/*n*1	*P*–1
Unit cell dimensions		
a (Å)	12.4222(3)	8.6122(5)
b (Å)	21.9259(5)	11.0090(8)
c (Å)	19.3284(4)	11.7897(8)
α (°)	90	81.7870(10)
β (°)	104.483(5)	73.517(9)
γ (°)	90	82.4940(10)
Volume/Å^3	5097.1(2)	1056.08(13)

Z	4	1
ρcalc (mg/mm^3)	1.575	1.547
Absorption coefficient (mm^{-1})	1.174	1.168
F(000)	2480	502
Crystal	Block; pale yellow	Plate; Blue
Crystal size (mm^3)	0.07 × 0.06 × 0.04	0.06 x 0.03 x 0.01
θ range for data collection (°)	2.367 – 27.483	2.461 – 27.543
Reflections collected	33878	13558
Independent reflections	11591	4792
Completeness to θ max (%)	99.8	99.2
Max and min transmission	1.000 and 0.811	1.000 and 0.694
Data/restraints/parameters	11591/ 0 / 745	4792 / 0 / 289
Goodness-of-fit on F2	1.025	1.080
Final R indexes [I>=2σ (I)]	*R1* = 0.0439, *wR2* = 0.0993	*R1* = 0.0813, *wR2* = 0.1082
Final R indexes [all data]	*R1* = 0.0647, *wR2* = 0.1078	*R1* = 0.1660, *wR2* = 0.1376
Largest diff. peak/hole (e Å-3)	1.695/ –0.688	0.584/ –0.623

Table 2 Selected bond lengths (Å) and bond angles (°) for complexes (**2**) and **(5)**

		2		**5**
M Bond Distances (Å)				
	Zn1–O1	2.059(2)	Cu1–O1	1.968(4)
M-O(C)	Zn1–O43	2.079(2)	Cu1–O3	1.961(4)
	Zn41-O3	2.057(2)		
	Zn41-O41	2.062(2)		
M-O(W)	Zn1-O1W	2.059(2)		
	Zn41-O2W	2.056(2)		
M-N(C)	Zn1–N 21	2.168(2)	Cu1–N21	1.996(5)
	Zn1-N22	2.094(2)	Cu1-N22	2.010(4)
	Zn41-N61	2.103(2)		
	Zn41-N62	2.159(2)		
S-S	S1–S2	2.061(1)		
	S41-S42	2.047(1)		
C-O	O1-C1	1.266(3)		
	O2-C1	1.251(3)		
Bond Angles(°)				
O-M-O	O1–Zn1–O1W	87.5(1)	O1–Cu1–O3	93.5(2)
	O1–Zn1–O43	93.0(1)	O1–Cu1–N21	164.4(2)
	O1W–Zn1–O43	150.2(1)		
O-M-N	O1–Zn1–N21	169.0(1)	O1–Cu1–N22	94.3(2)
	O1–Zn1–N22	92.9(1)	O3–Cu1–N21	93.4(2)
	O1W–Zn1–N21	87.8(1)	O3–Cu1–N22	168.1(2)
	O1W–Zn1–N22	102.3(1)		
	O43–Zn1–N21	96.0(1)		
	O43–Zn1–N22	107.5(1)		
N-M-N	N21–Zn1–N22	78.4(1)	N21–Cu1–N22	81.4(2)
C-S-C			C7–S1–C8	101.3(3)
Torsion Angles(°)				
C-S-S-C	C7–S1–S2–C8	-90.2(1)		
	C47–S41–S42–C48	-93.3(1)		

The coordination sphere around Zn(II) is composed of two carboxylate oxygens coming from two different disulfide ligands, one oxygen from water and two nitrogens from phenanthroline. The calculated τ_5 parameter value of 0.95 confirms that the Zn ion has a distorted trigonal

bypyramidal coordination environment ($\tau_5 = (\beta - \alpha)/60° \sim -0.01667\alpha + 0.01667\beta$ where $\beta > \alpha$ are the two greatest valence angles associated with the coordination centre) [31]. The Zn-O distances range between 2.057(2) - 2.079(2) Å and the values agree with those found in the literature [22, 32, 33]. The Zn-N bond lengths range between 2.094(2) - 2.168(2) Å which is close to reported Zn-bipyridine bond lengths [34, 35]. The S-S bond lengths are 2.047(1) - 2.061(1) Å which are similar to those in other disulfide ligands reported [17]. The O-Zn-O and O-Zn-N bond angles range from 87.5(1) to 150.2(1)°. Since the carboxylate oxygens have chelating ability, polymeric network results between the adjacent neighbours which form along crystallographic axis a (Figure 1b). The disulfide bridges lie on a horizontal axis, with the phen ligands orienting out of plane to minimize steric hindrance. The polymeric chains are held together by π-π stacking interactions which occur between the phen ligands and dtdb ligands or other phen ligands attributed to different chains. Hydrogen bonding between the chains also strengthens the arrangement (O1W-H1W···O42 and O2W-H2W···O44). Disordered DMF solvent molecules reside in the accessible free volume within the polymeric structure.

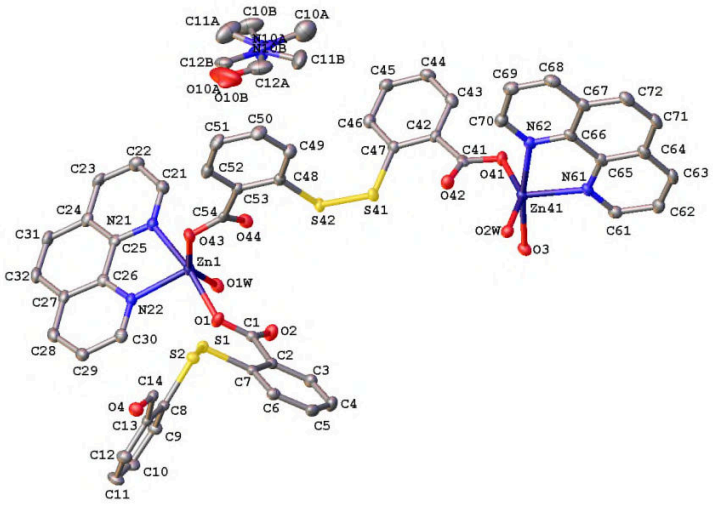

(a)

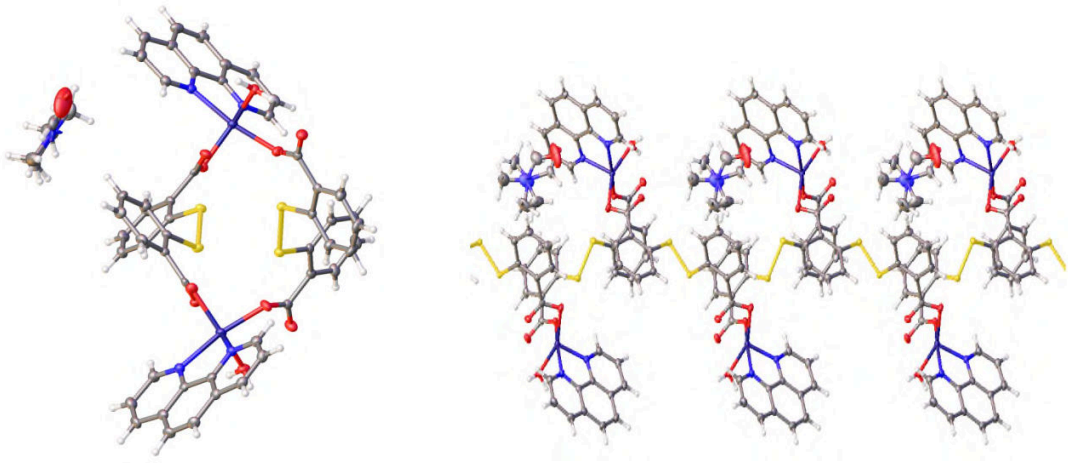

(b) **(c)**

Figure 1: (a) The X-ray crystal structure of (2), [Zn(dtdb)(phen)(H_2O)].DMF]. All hydrogen atoms are omitted for clarity. **(b) Packing viewed down crystallographic axis a. (c) Packing viewed down crystallographic axis c. Thermal ellipsoids are drawn at 50% probability level. (d) Colour code: red-oxygen, blue-nitrogen, yellow-sulfur and purple-zinc.**

Though various attempts were made to obtain X-ray diffraction data for complex (**3**) the quality of data was such that the full structure determination could not be solved. In spite of the low quality of the data obtained, a structure solution was obtained and it indicated the connectivity of the metal and detailed whether the dtdb ligand had once again formed as was observed for (**2**). The connectivity of the Co complex appeared to be consistent with what was observed for the Zn complex in the sense that it also had a distorted trigonal bipyramidal coordination environment. Each Co(II) appeared to be coordinated to two nitrogens from the phen moiety, one oxygen from water and two oxygens associated with two different dtdb ligands each bonded in a monodentate fashion. The formation of the S-S bond could also be seen. A disordered DMF molecule was also observed lying in a similar position. It is not possible to quote bond lengths or angles due to the poor quality of the data.

Complex (**5**) crystallizes in the triclinic space group *P-1*. The asymmetric unit comprises one Cu ion which is bonded to two nitrogen atoms from the bipy ligand and two oxygen atoms from the

carboxylate of two tdb moieties (Figure 2a). The Cu ion has a distorted square planar coordination environment. The molecule forms a dimer. The Cu-O and Cu-N bond lengths are 1.961 and 1.968(4) Å, and 1.996(5) - 2.010(4) Å respectively. The distortion in the square-based arrangement in complex **5** was evidenced by the variations in the two O-Cu-N bond angles [O1-Cu1-N21, 164.4(2)º; O1-Cu1-N22; 94.3(2)º]. The Cu-Cu distances are longer than the sum of van der Waals' radii, showing no interactions between the copper atoms. Each dimer is linked to another dimer through π-π stacking interactions which occur between the phen ligands, forming a 1D supramolecular network running along crystallographic axis b.

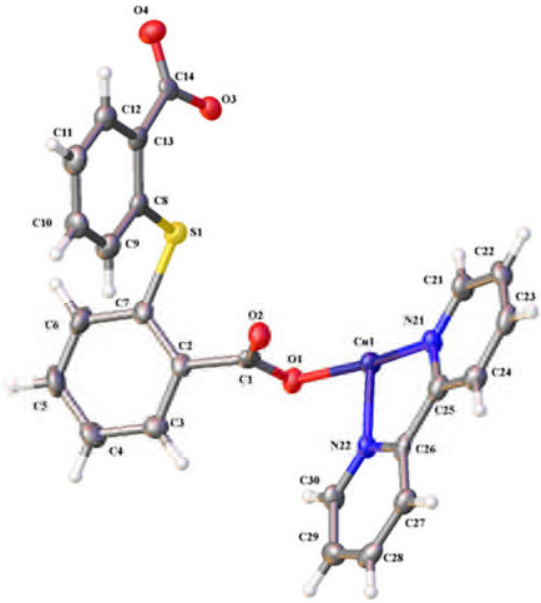

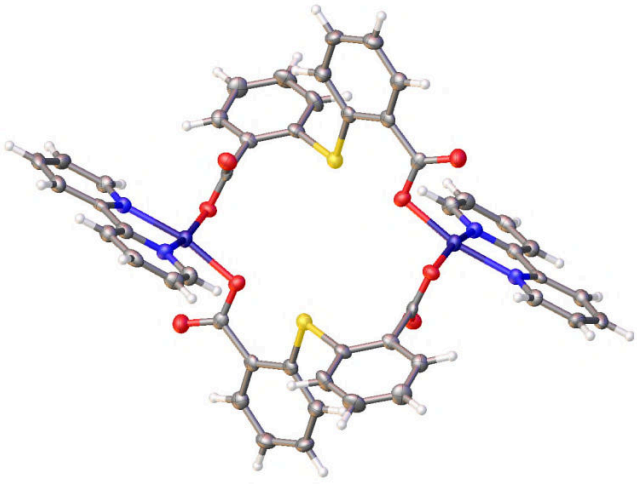

(a) **(b)**

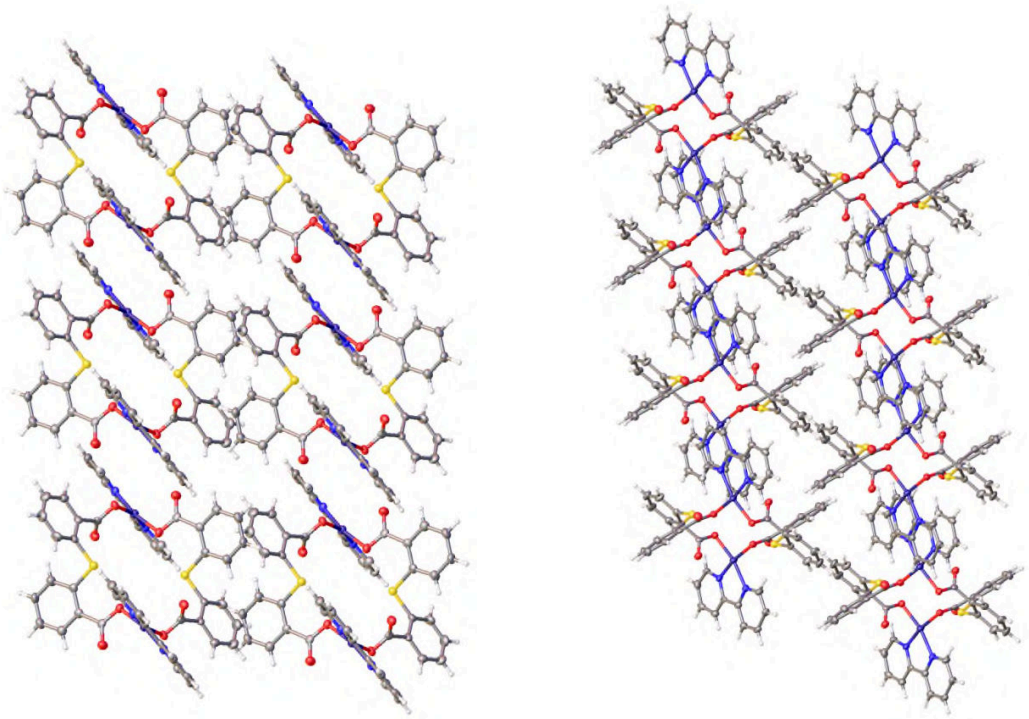

(c) **(d)**

Figure 2: The X-ray crystal structure of [Cu(tdb)(bipy)] (5). (a) Asymmetric unit (b) Dimer (c) Packing viewed down crystallographic axis a. (d) Packing viewed down crystallographic axis b. Thermal ellipsoids are drawn at 50% probability level. (e) Colour code: red-oxygen, blue-nitrogen, yellow-sulfur and purple-copper.

4.0 Conclusion

In this work, the reactions of different metals with thiosalicylic acid in the presence of N-donor ligands have been outlined systematically. Under the experimental conditions employed, the thiol group underwent facile oxidation to form the disulfide bridge which in turn coordinated with Zn, Co and Ni metal ions. In the case of ruthenium, the thiol ligand remained unchanged whilst in the presence of copper, thiol underwent oxidation followed by cleavage to form the thiodibenzoate ion prior to co-ordination. In all structural frameworks, the coordination was exclusively through the carboxylate groups, except in the ruthenium complex where both the hard oxygen and soft sulfur atoms were involved in bonding.

Supplementary Information

Crystallographic data for the structural analyses of complexes **2** and **5** have been deposited at the Cambridge Crystallographic Data Centre, bearing the CCDC Nos. 1499583 and 1410727 respectively.

References

[1] C. C. Eichman, J. P. Stambuli, *Molecules* **2011**, *16*, 590.

[2] D. Stibal, B. Therrien, F. Giannini, L. E. Paul, J. Furrer, G. Süss-Fink, *Eur. J. Inorg. Chem*. **2014**, 5925.

[3] F. Giannini, M. Bartoloni, L. E. H. Paul, G. Süss-Fink, J. L. Reymond, J. Furrer, *Med. Chem. Comm*. **2015**, 347.

[4] T. Wehr-Candler, W. Henderson, *Coord. Chem. Rev.* **2016**, *313***,** 111.

[5] A. Majumdar, K. Pal, S. Sarkar. *Dalton Trans*. **2009**, *21*, 1927.

[6] J. S. Bashkin, J. C. Huffman, G. A. Christou, *J. Am. Chem. Soc*. **1986**, *108*, 5038.

[7] R. C. Bott, P. C. Healy, D. S. Sagatys, *Chem. Commun*. **1998**, 2403.

[8] D. Cave, J-M. Gascon, A. D. Bond, S. J. Teat, P. T. Wood, *Chem. Commun*. **2002**, *10* 1050.

[9] Z. L. Wang, L. H. Wei, M. X. Li, J. P. Wang, *Chinese J. Struct. Chem*. **2008**, *27*, 1327.

[10] F. E. Jacobsen, S. M. *Inorg. Chem*. **2004**, 43, 3038.

[11] W. Henderson, B. K. Nicholson, A. G. Oliver, C. E. Rickard, *J. Organomet. Chem.* **2001**, *625,* 40.

[12] S. L-F. Chan, R. W-Y. Sun, M-Y. Choi, Y. Zeng, L. Shek, S. S-Y. Chui, C-M. Che, *Chem. Sci*. **2011**, *2*, 1788.

[13] S. L-F. Chan, G. Song, S. S-Y. Chui, L. Shek, J-S., Huang, C-M. Che, *Chem. Eur. J.* **2012**, 18, 11228.

[14] J. Wagner, P. Vitali, J. Schoun, E. Giroux, *Can. J. Chem*. **1977***, 55*, 4028.

[15] E. Block, V. Eswarakrishnan, M. Gernon, G. Ofori-Okai, C. Saha, K.Tang, J. Zubieta, *J. Am. Chem. Soc.* **1989**, *111*, 658-665.

[16] C. E. Rowland, P. M. Cantos, B. H. Toby, M. Frisch, J. R. Deschamps, C. L. Cahill, *Cryst. Grow. Des.* **2011**, *11,* 1370.

[17] R. Murugavel, K. Baheti, G. Anantharaman, *Inorg. Chem.* **2001,** *40*, 6870.

[18] S. J. Coles, P. A. Gale, *Chem. Sci.* **2012**, *3*, 683.

[19] C. S. Rigaku. 2015. Expert 3.1, b27;(c) Sheldrick. *Acta Crystallogr*. C, **2013**, *71***.**

[20] L. Palatinus, G. Chapuis, *J. Appl. Crystallogr.* **2007**, *40*, 786.

[21] G. M. Sheldrick, *Acta Crystallogr. Sect. A* **2008**, *64*, 112.

[22] O. V. Dolomanov, L. J. Bourhis, R. J. Gildea, J. A. Howard, H. Puschmann, *J. Appl. Crystallogr.* **2009**, *42*, 339.

[23] S. B. Moosun, L. H. Blair, S. J. Coles, M. G. Bhowon, S. Jhaumeer-Laulloo, *Trans. Met. Chem.* **2015**, 40, 161.

[24] S. Moosun, J. A. Joule, M. G. Bhowon, S. Jhaumeer-Laulloo, *Phosphorus Sulfur Silicon Relat. Elem.* **2012**, *187*, 1383.

[25] Y. M. Dai, J. F. Huang, H. Y. Shen. *Acta Crystallogr. Sect. E* **2005**, *E61*, m2491.

[26] S. M. Humphrey, R. A. Mole, J. M. Rawson, P. T. Wood, *Dalton Trans.* **2004**, *11*, 1670.

[27] B. S. Kusmariya, A. Tiwari, A. P. Mishra G. A. Naikoo, *J. Mol. Struct.* **2016**, *11*, 115.

[28] S. K. Ahmed, S. Khaled *Arabian J. Chem. in press* **2015:**http://dx.doi.org/10.1016/j.arabjc.2015.04.025

[29] S. B. Moosun, L. H. Blair, S. J. Coles, S. J. Laulloo, M. G. Bhowon, *Z. Anorg. Allg. Chem.* **2015**, *5*, 890-895.

[30] S. Liu, X. Z. Li. *Kristallogr. New Cryst. Struct.* **2010**, *225*, 194.

[31] L. Yang, D. R. Powell, R. P. Houser, *Dalton Trans*. **2007**, *9*, 955.

[32] J. He, Y. Wang, W. Bi, X. Zhu, Cao, R. *J. Mol. Struct*. **2006**, *787*, 63.

[33] M. R. Rizal, S. W. Ng *Acta Crystallogr Sect. E* **2009**, *65,* m1178.

[34] D. Chen, Y. Wang, Z. Lin, F. Huang. *J. Mol. Struct*. **2010**, *966*, 59.

[35] Y. Q. Zheng, W. Liu, F. Y. Yao. *J. Coord. Chem*. **2009**, *62,* 2497.

Formation and Structural Characterization of Metal Complexes derived from Thiosalicylic acid

Bhowon, Minu G.

2017-09-01

Bhowon MG, Jhaumeer-Laulloo S, Moosun S, et al., (2017) Formation and Structural Characterization of Metal Complexes derived from Thiosalicylic acid. Journal of Inorganic and General Chemistry / Zeitschrift für anorganische und allgemeine Chemie, Volume 643, Issue 18, October 2017, pp. 1167-1172

https://doi.org/10.1002/zaac.201700244